ELSEVIER

Journal of Biomechanics 38 (2005) 1517–1525

JOURNAL OF BIOMECHANICS

www.elsevier.com/locate/jbiomech
www.JBiomech.com

Fracture in human cortical bone: local fracture criteria and toughening mechanisms

R.K. Nalla[a], J.S. Stölken[b], J.H. Kinney[b], R.O. Ritchie[a,*]

[a]*Materials Sciences Division, Lawrence Berkeley National Laboratory, and Department of Materials Science and Engineering, University of California, Berkeley, CA 94720 USA*
[b]*Lawrence Livermore National Laboratory, Livermore, CA 94550*

Accepted 19 July 2004

Abstract

Micromechanical models for fracture initiation that incorporate local failure criteria have been widely developed for metallic and ceramic materials; however, few such micromechanical models have been developed for the fracture of bone. In fact, although the fracture event in ''hard'' mineralized tissues such as bone is commonly believed to be locally strain-controlled, only recently has there been experimental evidence (using double-notched four-point bend testing) to support this widely held belief. In the present study, we seek to shed further light on the nature of the local cracking events that precede catastrophic fracture in human cortical bone, and to define their relationship to the microstructure. Specifically, numerical computations are reported that demonstrate that the stress and strain states ahead of such a notch are *qualitatively* similar irrespective of the deformation mechanism (pressure-insensitive plasticity vs. pressure-sensitive microcracking). Furthermore, we use the double-notched test to examine crack–microstructure interactions from a perspective of determining the salient toughening mechanisms in bone and to characterize how these may affect the anisotropy in fracture properties. Based on preliminary micromechanical models of these processes, the relative contributions of various toughening mechanisms are established. In particular, crack deflection and uncracked-ligament bridging are identified as the major mechanisms of toughening in cortical bone.

Keywords: Bone; Fracture; Toughening; Microstructure

1. Introduction

Recent interest in bone and its mechanical properties has led to extensive research into how it fractures (e.g., Lindahl and Lindgren, 1967; Burnstein et al., 1976; Wright and Hayes, 1976; Katz, 1980; Ashman and Rho, 1988; Park and Lakes, 1992; Keaveny et al., 1994; Vashishth et al., 1997; Zioupos and Currey, 1998; Burr, 2002; Nalla et al., 2003a), although several questions remain unaddressed. For example, although models for bone fracture are invariably based on the concept of a strain-controlled critical fracture event (e.g., Keaveny et al., 1994; Ford and Keaveny, 1996; Yeh and Keaveny, 2001), until recently (Nalla et al., 2003a) there has been no experimental evidence to verify this hypothesis. Specifically, the experimental verification of strain-controlled fracture initiation in bone was achieved using a double-notched four-point bend test. The basis of this test is two-fold: (i) since both notches experience the same bending moment, when one notch breaks, the other is ''frozen'' at the point of fracture, and (ii) in the presence of any degree of inelasticity, the maximum stresses peak ahead of the notch whereas the maximum strains are at the notch. Consequently, microstructural examination of the unbroken notch can give insight into cracking events immediately preceding fracture; in particular, the location of the microstructural cracking event that precedes macroscopic fracture at a notch

*Corresponding author. Tel.: +1-510+486-5798; fax: +1-510-486-4881.
E-mail address: roritchie@lbl.gov (R.O. Ritchie).

0021-9290/$ - see front matter © 2004 Elsevier Ltd. All rights reserved.
doi:10.1016/j.jbiomech.2004.07.010

gives a definitive indicator of whether fracture initiation is locally stress- or strain-controlled. Strain-controlled fracture will initiate at the notch whereas stress-controlled will initiate ahead of the notch. Preliminary experiments on human cortical bone (Nalla et al., 2003a) (and also on human dentin (Nalla et al., 2003b) showed that the initial *local* fracture events do indeed initiate at the notch in both materials, which is consistent with a strain-based failure mechanism.

The notch-field stress and strain distribution used in these studies (Hill, 1950; Griffiths and Owen, 1971), however, pertained to a Mises solid, i.e., based on pressure-insensitive plasticity as in metals, whereas inelasticity in bone may involve pressure-insensitive mechanisms such as plasticity in the collagen fibers and pressure-sensitive mechanisms such as microcracking (Currey, 2001; Taylor, 2003), where the corresponding notch solutions are unknown. Consequently, in this work, we determine the stress distributions using finite-element analysis for both pressure-insensitive plasticity and pressure-sensitive microcracking, with the objective of further developing the double-notch test to probe the *local* fracture events in bone. We use the technique to seek further understanding of (i) the criteria for crack initiation, and (ii) the salient toughening mechanisms associated with subsequent crack growth and how they are affected by the hierarchical microstructure of bone. To date, although various toughening mechanisms have been proposed, including microcracking, crack deflection and crack bridging (e.g., Vashishth et al., 1997, 2000; Yeni and Norman, 2000; Parsamian and Norman, 2001; Thompson et al., 2001; Yeni and Fyhrie, 2001; Wang et al., 2001, 2002; Nalla et al., 2003a, 2004, 2005), little definitive information exists for their relative potency. Moreover, as they undoubtedly operate *in concert*, this almost certainly controls the orientation-dependence of the toughness with respect to the microstructure. Consequently, we also seek to investigate how microstructure affects this anisotropy of fracture toughness by quantifying the effect of these mechanisms by simple theoretical modeling.

2. Methods and materials

2.1. Numerical computations

Events that result in macroscopic fracture can be described as either locally *stress-* or *strain-controlled*. To derive the stress/strain distributions required to achieve this distinction, numerical analysis using the nonlinear, implicit, three-dimensional finite-element code NIKE3D (Maker and Hallquist, 1995) was used to simulate inelastic deformation ahead of a notch in plane-strain. Using symmetry, only one quadrant of the problem was modeled with a 4000 linear finite element graded mesh. The region simulated extended over a distance equivalent to 100 times the notch radius in both directions. Uniaxial displacement was applied along the upper boundary. Infinite-body conditions were approximated by constraining the edge of the region to move with parallel motion.

To simulate deformation by pressure-insensitive plasticity and pressure-sensitive microcracking, two nonlinear materials models were used. The first "plastic-damage" model (PD) used a Mises yield criterion, based on tissue material properties provided by Niebur et al. (2000). At stresses beyond the yield stress, the material becomes perfectly plastic; plastic strain was accumulated without change in unloading modulus. An isotropic Young's modulus of 18.7 GPa was assumed. The second model, utilized to better simulate deformation by microcracking, was based on the oriented "brittle-damage" model (BD) of Govindjee et al. (1995). This model treats the compliance tensor as an internal variable, and adopts the maximum damage-dissipation principle (Simo and Ju, 1987) (equivalent to the maximum plastic-work principle in models of associative-plasticity). In compression, the constituent response was taken to be plastic yielding (identical to PD model); in tension, a smeared-crack model was used to simulate damage evolution. This has the effect of reducing the element stiffness in response to an increased microcrack density, the growth of which is controlled by the toughness. A fracture toughness, $K_c = 3.2\,\mathrm{MPa}\sqrt{\mathrm{m}}$ (strain-energy release rate $\sim 500\,\mathrm{J/m^2}$) was selected from the middle of the range of toughnesses for bone (Zioupos and Currey, 1998; Lucksanambool et al., 2001; Phelps et al., 2000). As microcracking damage was considered to be unrecoverable, this reduced the unloading modulus. The damage threshold for microcrack nucleation was taken to be 0.6% strain. Both models are fully described by Stölken and Kinney (2003).

2.2. Experimental fracture testing

Human cortical bone from the mid-diaphyses of three freshly frozen cadaveric humeri (from 34-year old females) was used; three orientations were studied (Fig. 1):

- *anti-plane longitudinal* (*medial–lateral*)— long axes of the osteons in the plane of the notch/crack, but perpendicular to the (nominal) crack-propagation direction ($N = 9$),
- *in-plane longitudinal* (*proximal–distal*)— long axes of the osteons in the plane of the notch/crack, but perpendicular to the crack-propagation direction ($N = 7$),
- *transverse*— long axes of the osteons perpendicular to the plane of the notch/crack and to the crack-propagation direction ($N = 6$).

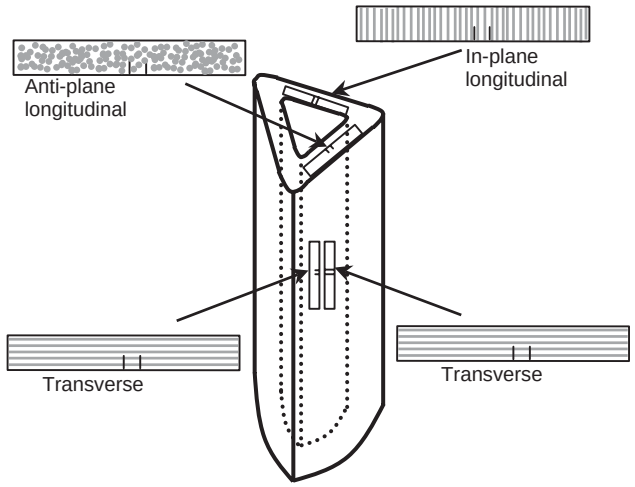

Fig. 1. Schematic illustration of the various specimen orientations, namely transverse, proximal–distal (in-plane longitudinal) and medial–lateral (anti-plane longitudinal), taken from the humeri (with respect to the direction of the osteons, indicated in gray).

Experiments on $N = 22$ samples (thickness B~1.1–2.6 mm, width W~1.7–2.7 mm, spacing between inner loading points S~10–15 mm, notch root-radius ρ~200–300 μm, notch depth a/W~0.3–0.4) were performed using the double-notched four-point bending geometry, as this enabled a determination of whether crack initiation was stress- or strain-controlled and further permitted the development of stable cracks. Samples were kept hydrated during fabrication; prior to testing, they were soaked in 25 °C Hanks' balanced salt solution (HBSS) in air-tight containers for 40 h[1].

All testing was conducted in 25 °C HBSS using an ELF® 3200-series mechanical-testing machine; bend bars were loaded under displacement control at a constant displacement rate of 0.01 mm/s. The area around the unfractured notch in failed double-notched samples was examined using optical microscopy and, after coating with gold-palladium, in a scanning electron microscope (SEM) operating in the back-scattered electron mode.

Additional fracture-toughness tests were conducted using the three-point-bending geometry (B~1.1–2.6 mm, W~1.7–2.7 mm, $S = 5.0-5.5\,W$) in the three orientations ($N = 3$ for each orientation). A fatigue precrack was grown from the notch at a load ratio (ratio of minimum-to-maximum loads) of $R = 0.1$ at 2 Hz frequency; the final maximum stress intensity was 1–2 MPa$\sqrt{}$m with final precrack length of 0.4–0.6 W. Samples were loaded to failure under displacement control in 25 °C HBSS at a cross-head displacement rate of 0.01 mm/s, with applied loads and load-line displacements simultaneously monitored in situ. Stress-intensity factors, K, were computed from handbook solutions (ASTM Standard E-399-90, 2001). Due to substantial crack deflections, mode-I stress intensities for the transverse orientation may be somewhat questionable. Consequently, additional measurements were made of the work-of-fracture, W_f, an alternative measure of toughness obtained by dividing the area under the load–displacement curve by twice the nominal crack-surface area; however, this latter parameter is both size- and geometry-dependent.

3. Results

3.1. Numerical computations

Normalized notch-field stress/strain distributions from the finite-element simulations are shown in Fig. 2. For both models of inelasticity, i.e., the plasticity (PD)

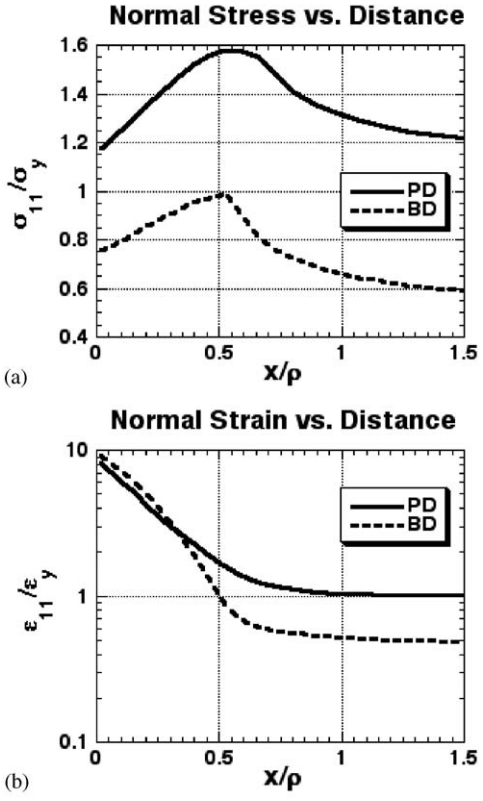

Fig. 2. Non-linear, finite-element computations of the distributions of (a) tensile stress, σ_{11}, and (b) strain, ε_{11}, normalized by the yield stress, σ_y, and yield strain, ε_y, respectively, as a function of distance, x, ahead of a round hole, normalized by the radius of the notch, ρ. Calculations are shown for inelastic deformation based on classical pressure-insensitive, shear-driven plastic deformation (PD) model and pressure-sensitive microcracking (brittle damage—BD) model.

[1]It is possible that degradation of the collagen and/or leaching of the mineral into solution could alter properties with time. However, no such changes could be detected in parallel investigations in dentin following short-time storage under identical conditions (Habelitz et al., 2002).

and brittle-damage (BD) models, the stresses peak *ahead* of the notch whereas the strains peak directly *at* the root of the notch. Thus, both distributions are qualitatively similar for materials undergoing either shear-driven (pressure-insensitivity) plasticity, e.g., as in metals, or pressure-sensitive microcracking. These results are consistent with those for J2 plasticity (Hill, 1950; Griffiths and Owen, 1971) and with experimentally measured crack-tip strain distributions reported by Nicolella et al. (2001) for bone. Thus, the double-notched-bend technique can be used to distinguish between stress- and strain-controlled fracture in terms of where cracking first initiates in materials undergoing both forms of "yielding", namely shear-driven plastic-flow and pressure-sensitive microcracking. This result validates the use of the double-notch test for this purpose in mineralized tissue materials such as bone.

3.2. Fracture testing

Crack initiation: Consistent with the preliminary data of Nalla et al. (2003a), results from the double-notched four-point-bend tests showed that without exception, all precursor cracks formed directly at the notch root; there was no evidence of precursor cracking at the site of maximum stress (Fig. 3). This provides experimental verification to endorse the concept that crack initiation in human cortical bone is locally strain-controlled. In the transverse orientation, i.e., how bone typically fails in vivo, in addition to incipient cracking at the notch root, there are instances of crack formation at microstructural features, such as the Haversian canals, near the notch (Fig. 3d), consistent with the higher strains measured at such features (Nicolella et al., 2001).

Crack growth: With respect to crack growth, it is evident from Fig. 3 that the underlying microstructure has a marked influence on the nature of the crack path, particularly in the transverse orientation. Whereas fracture in the longitudinal orientations (Figs. 3a,b) nominally follows an expected trajectory dictated by the path of maximum tensile stresses, cracks in the transverse orientation extend initially in an unlikely direction perpendicular to the notch (Figs. 3c, d).

SEM micrographs of the subsequent propagation of such cracks are shown in Fig. 4. Fig. 4a shows the relatively deflection-free trajectory of a ~1 mm long crack in the medial–lateral orientation. However, crack/microstructural interactions are evident in other orientations, which leads to toughening. Figs. 4b,c show evidence of so-called *uncracked-ligament bridging*, an extrinsic-toughening mechanism involving two-dimensional uncracked regions along the crack path that can bridge the crack on opening. This mechanism, which is commonly seen in metal–matrix composites (Shang and Ritchie, 1989) and intermetallics (Campbell et al., 1999), is often the result of either the non-uniform advance of

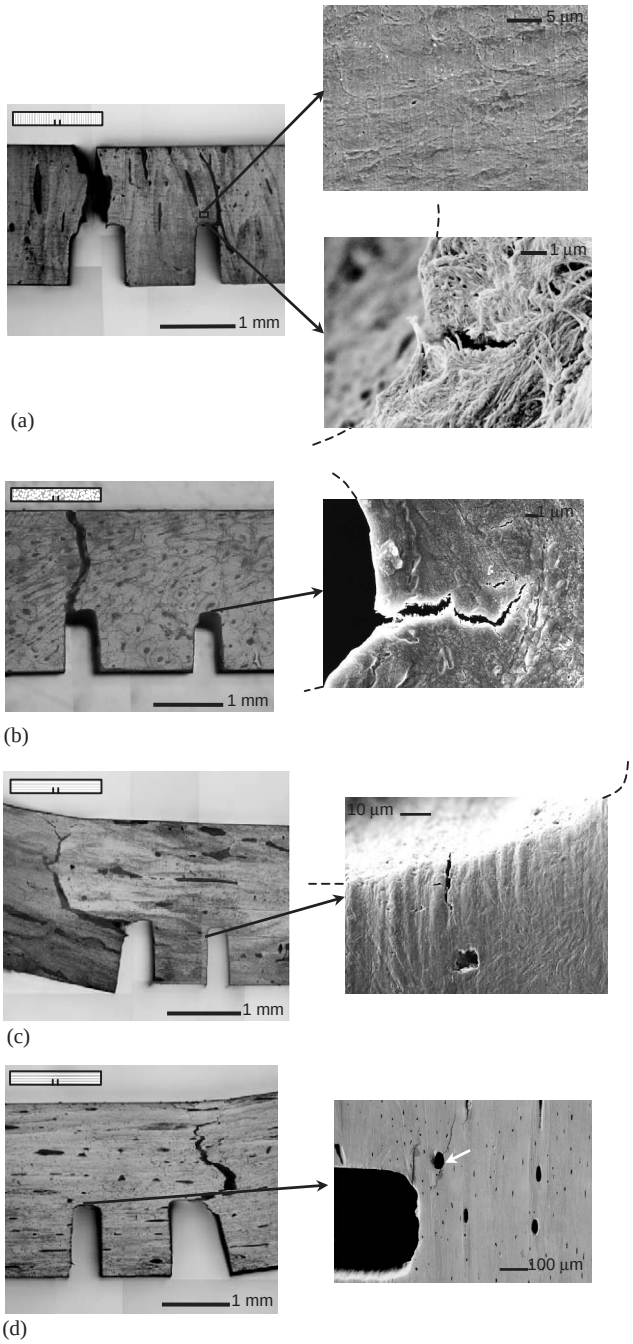

Fig. 3. Optical micrographs (left) of typical double-notch specimens after fracture, together with scanning electron micrographs (right) of the area of interest for the purpose of determining the failure criterion. Note the absence of crack initiation at the location of maximum stress as illustrated for the in-plane longitudinal (proximal–distal) orientation (a: top, right). A much stronger influence of the underlying microstructure can be seen for the transverse orientations (c and d) as compared to the longitudinal ones (a and b). Also, for the transverse orientation, in some instances, cracking was observed ahead of the notch at a Haversian canal (d). The schematic insets in each optical micrograph show the orientation of the specimen and the black dashed lines (in a–c) indicate the notch surface.

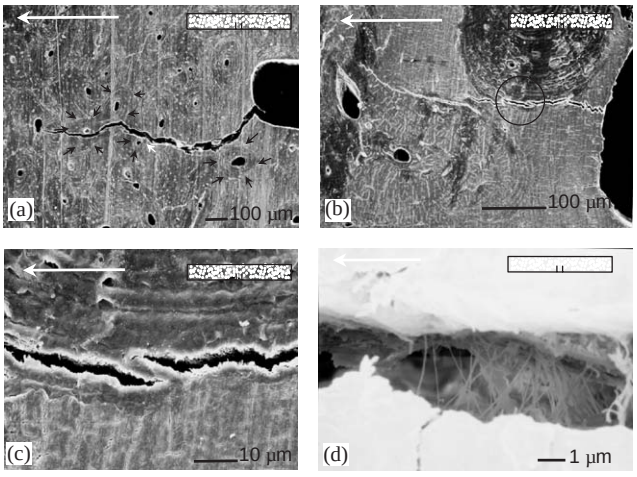

Fig. 4. Scanning electron micrographs illustrating crack–microstructure interactions. For the anti-plane longitudinal (medial–lateral) orientation, (a) the secondary osteons (indicated by black arrows) have a weak influence on crack path (after Nalla et al., 2003a), (b) evidence of bridging due to a secondary lamella, also shown at higher magnification in (c), and (d) possible collagen fibril-based bridging. The insets show the specimen orientation used and the white arrows in (a–d) indicate the direction of nominal crack growth.

the crack front and/or the imperfect link-up of microcracks initiated ahead of the crack tip with the main crack. Uncracked-ligament bridging and microcracking in the vicinity of the crack are also seen in the proximal–distal orientation (Nalla et al., 2003a). The microcracking can in principle lead to extrinsic toughening since it can cause dilation and increase the compliance of the region surrounding the crack. In addition, crack bridging by individual collagen fibrils may provide further toughening (Fig. 4d).

However, the largest microstructural influence on the crack path can be seen in the transverse orientation, where secondary osteons run along the specimen length. As mentioned previously, crack initiation and initial crack growth out of the notch did not occur on a plane normal to the maximum tensile stress, but rather perpendicular to this in the nominal direction of the osteon system (Fig. 3c). As suggested by Yeni and Norman (2000), it appears that the initiated crack can be deflected from the nominal direction of propagation along the cement lines that are the interfaces between the secondary osteons and the surrounding matrix as this provides a weaker path away from the path of maximum tensile stress. Indeed, although there is significant cracking ahead of the notch at a Haversian canal (indicated by white arrow) in Fig. 3d, this seems to be ignored by the main crack at the notch. The marked (~90°) deflections in crack path seen in this case can lead to substantial toughening and may be the major factor contributing to the anisotropy in fracture properties in bone.

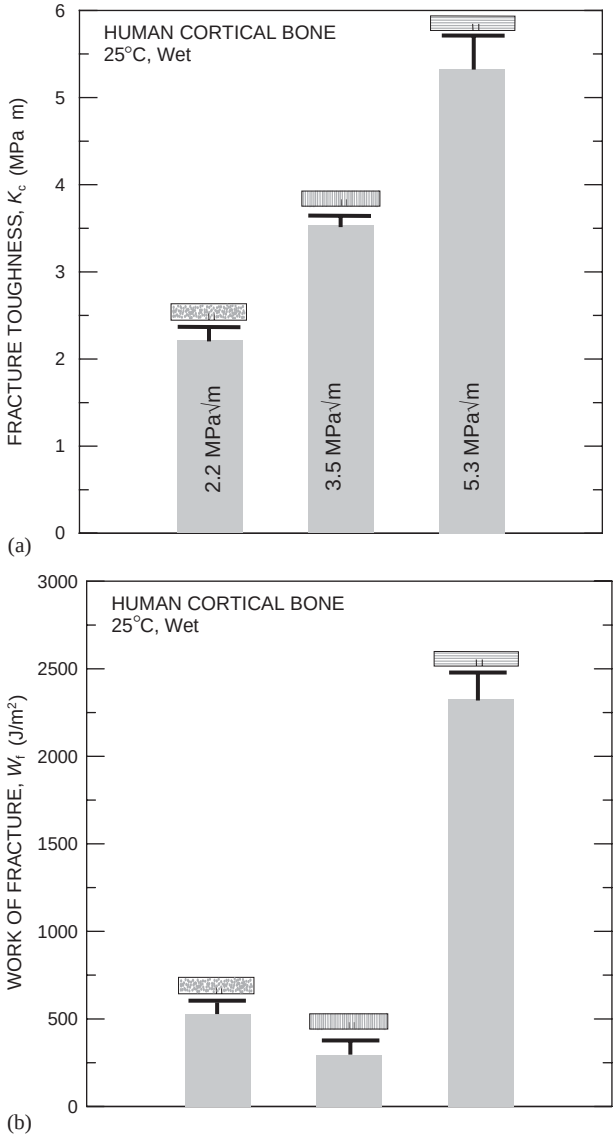

Fig. 5. The measured toughness of bone, in terms of (a) fracture toughness and (b) work of fracture results, obtained in this study for different orientations (schematically shown) with respect to the osteons. The half-error bars indicate one standard deviation; the numbers in (a) are the average toughness values.

The measured fracture-toughness and work-of-fracture values, given in Fig. 5 show K_c to be 2–6 MPa$\sqrt{m}$, i.e., consistent with the previous results of Zioupos and Currey (1998), Lucksanambool et al. (2001), and Phelps et al. (2000). In terms of K_c values, the transverse orientation is between 51–140% tougher than the longitudinal orientations. However, since the K_c values in the transverse orientation may be somewhat questionable, work-of-fracture measurements are also shown and indicate a toughness in the transverse orientation that is again far in excess of the corresponding values for either of the longitudinal orientations; similar qualitative trends have been reported by Lucksanambool et al. (2001). Such *measured* anisotropy in toughness is

believed to be a direct result of the various active toughening mechanisms, namely crack bridging, crack deflection and microcracking. While such mechanisms have long been hypothesized in bone (e.g., microcracking by Vashishth et al. (1997, 2000), Parsamian and Norman (2001); crack deflection by Yeni and Norman (2000); collagen fiber bridging by Thompson et al. (2001), Wang et al. (2001, 2002), Yeni and Fyhrie (2001); and uncracked-ligament bridging by Nalla et al. (2003a, 2004, 2005)), evidence of their *quantitative* relevance has largely been lacking; this issue is addressed below.

4. Discussion

The microstructure of a material can influence the fracture toughness in two primary ways (Ritchie, 1988, 1999):

- it can affect the inherent resistance to microstructural damage and fracture *ahead* of the crack tip, which is termed *intrinsic toughening*, and/or
- it can promote crack-tip shielding, i.e., act to reduce the local stress intensity actually experienced *at or behind* the crack tip, which is termed *extrinsic toughening*.

Crack propagation can be considered as a mutual competition between these two classes of mechanisms, i.e., microstructural damage in the process zone ahead of the crack tip, which acts to promote crack extension, and extrinsic crack-tip shielding behind the tip, which acts to impede it. Whereas intrinsic toughening tends to dominate in ductile materials and to affect crack-initiation resistance, extrinsic mechanisms are invariably the main source of toughening in brittle materials, and govern crack-growth resistance. Given the relatively brittle nature of bone and the nature of the crack–microstructure interactions (see Section 3.2), extrinsic mechanisms appear to provide the principal contributions to the toughness of bone, akin to other mineralized tissues such as dentin in vitro (Nalla et al., 2003c).

In the present work, firstly in terms of intrinsic damage, we have provided sound evidence that the onset of fracture in human cortical bone is consistent with a *strain-based* criterion, which has been so widely used in theoretical models of the mechanical behavior of bone (Keaveny et al., 1994; Ford and Keaveny, 1996; Yeh and Keaveny, 2001). Secondly, in terms of the salient toughening mechanisms, it is apparent from the current observations of the microstructural crack paths that this toughening arises extrinsically from several distinct sources:

- crack bridging by uncracked ligaments
- crack bridging by intact collagen fibrils
- macroscopic crack deflection
- microcracking.

Since the potency of these mechanisms depends on specific microstructural features, which in turn vary with orientation, the marked anisotropy in the fracture toughness can be considered to result directly from the relative contributions of these mechanisms.

The influence of the microstructure is strongest for the cracks growing transversely. This is believed to be the result of crack deflection along the cement lines, which offers a path of lower resistance. For cracks growing longitudinally, the osteons do not seem to influence the macroscopic crack growth substantially (Fig. 4a) (see also Nalla et al., 2004). This is reflected in the measured fracture-toughness results, which also display a marked orientation-dependence.

The highest toughness was observed in the transverse orientation, consistent with previous results (Lucksanambool et al., 2001; Phelps et al., 2000; Behiri and Bonfield, 1989); here the crack path deflects at $\sim 90^\circ$ to the plane of maximum tensile stress (Figs. 3c,d). The effect of this deflection is to increase the toughness substantially, as shown by the following analysis. Assuming, for the sake of simplicity, that these deflections/kinks represent in-plane tilts through an angle, α, to the crack plane, then the local mode-I and mode-II stress intensities, k_1 and k_2, at the deflected crack tip are given by (Bilby et al., 1978; Cotterell and Rice, 1980)

$$k_1(\alpha) = c_{11}(\alpha)K_{\mathrm{I}} + c_{12}(\alpha)K_{\mathrm{II}},$$

$$k_2(\alpha) = c_{21}(\alpha)K_{\mathrm{I}} + c_{22}(\alpha)K_{\mathrm{II}}, \quad (1)$$

where $K_{\mathrm{I}}(=5.33\,\mathrm{MPa}\sqrt{\mathrm{m}})$ and $K_{\mathrm{II}}(=0)$ are, respectively, the mode-I and mode-II far-field stress intensities for a main crack, and the coefficients, $c_{ij}(\alpha)$, are mathematical functions of the deflection angle, $\alpha(\sim 90^\circ)$ (Bilby et al., 1978; Cotterell and Rice, 1980). The effective stress intensity at the tip of the deflected crack tip, K_{d}, can then be calculated by summing the mode-I and mode-II contributions in terms of the strain-energy release rate, viz.:

$$K_{\mathrm{d}} = (k_1^2 + k_2^2)^{1/2}, \quad (2)$$

which suggests that the value of the stress intensity at the crack tip is reduced locally by $\sim 50\%$ due to such deflection to $\sim 2.7\,\mathrm{MPa}\sqrt{\mathrm{m}}$, compared to that for an undeflected crack. This calculation is consistent with the toughness being approximately twice as high in this orientation as compared to the longitudinal orientations.

In the proximal–distal and medial–lateral orientations, conversely, crack bridging appears to be the prominent source of toughening. Theoretical estimates

of bridging due to uncracked ligaments in the latter orientation can be made based on a limiting crack-opening approach (Shang and Ritchie, 1989) :

$$K_{\mathrm{br}} = \frac{-f_{\mathrm{ul}} K_{\mathrm{I}}[(1 + l_{\mathrm{ul}}/rb)^{1/2} - 1]}{1 - f_{\mathrm{ul}} + f_{\mathrm{ul}}(1 + l_{\mathrm{ul}}/rb)^{1/2}}, \quad (3)$$

where f_{ul} is the area-fraction of bridging ligaments on the crack plane (~0.2–0.4, from crack-path observations), K_{I} is the applied stress intensity (2.4 MPa$\sqrt{\mathrm{m}}$), l_{ul} is the bridging-zone size (~50–300 μm, from crack-path observations), r is a rotational factor (0.20–0.47) and $b = W - a$. Again, substituting typical values for these parameters, a contribution to the toughness on the order of K_{br}~0.3 MPa$\sqrt{\mathrm{m}}$ was obtained for the medial–lateral (anti-plane longitudinal) orientation. Similar analyses for the proximal–distal (in-plane longitudinal) orientation yielded even higher values of ~1–1.6 MPa$\sqrt{\mathrm{m}}$ due to the larger (~mm) bridging zones in this orientation (Nalla et al., 2004)

For toughening associated with bridging by collagen fibrils, the uniform-traction Dugdale-zone model (Evans and McMeeking, 1986) can be employed to estimate the resulting decrease in the stress intensity, $K_{\mathrm{b}}^{\mathrm{f}}$, due to "fiber-bridging", viz:

$$K_{\mathrm{b}}^{\mathrm{f}} = 2\sigma_{\mathrm{b}} f_{\mathrm{f}} (2l_{\mathrm{f}}/\pi)^{1/2}, \quad (4)$$

where σ_{b} is the normal bridging stress on the fibrils (~100 MPa), f_{f} is the effective area-fraction of the collagen fibrils on the crack plane (~0.15, from crack-path observations), and l_{f} is the bridging-zone length (~10 μm, from crack-path observations). Using these estimates, a value of $K_{\mathrm{b}}^{\mathrm{f}}$~0.08 MPa$\sqrt{\mathrm{m}}$ can be obtained for both longitudinal orientations where such bridging was observed, suggesting that bridging by individual collagen fibers contributes little to the toughness of bone. However, this mechanism might be expected to be significant for individual microcracks, where due to the substantially smaller size-scales collagen bridges would be able to span a larger percentage of the crack length.

Finally, based on accepted models for microcrack toughening due to dilation and modulus reduction (Evans and Faber, 1984; Hutchinson, 1987; Sigl, 1996), the increase in toughness due to microcracks can be expressed as

$$K_{\mathrm{m}} = 0.22\varepsilon_{\mathrm{m}} E' f_{\mathrm{m}} \sqrt{l_{\mathrm{m}}} + \beta f_{\mathrm{m}} K_{\mathrm{c}}, \quad (5)$$

where ε_{m} is the residual volumetric strain (=0.002, as calculated from data in Sigl, 1996), E' is the plane-strain elastic modulus, f_{m} is the volume-fraction of microcracks, l_{m} is the height of the microcrack zone, β is a factor dependent on Poisson's ratio (~1.2 (Sigl, 1996)[2].

[2]Note that the value of ε_{m} used will tend to overestimate the toughening since ε_{m} is directly proportional to the residual stresses in the material, which can be hundreds of MPa in ceramics, much higher than could be sustained in bone.

Using a volume-fraction, f_{m}~3% from present observations and those of Vashishth et al. (1997) for the in-plane longitudinal orientation, the contribution to the toughness from microcracking would be ~0.1 MPa$\sqrt{\mathrm{m}}$; similar values are obtained for the other orientations. As impractically high microcrack volume-fractions of ~60–90% would be needed for this mechanism to account for the observed toughness of bone (Nalla et al., 2004), we do not believe that constrained microcracking is a significant toughening mechanism.

In summary, direct experimental evidence has been presented in support of a *strain-controlled* mechanism for the onset of fracture in bone. In addition, a series of extrinsic toughening mechanisms have been identified, specifically crack bridging by uncracked ligaments and collagen fibrils, crack deflection, and microcracking, based on microscopic observations of the interaction of the crack path with the underlying microstructure. Using simple theoretical modeling for quantification, the dominant toughening mechanisms are deemed to be (i) crack deflection along the cement lines in the transverse orientation, and (ii) crack bridging by uncracked ligaments in the longitudinal orientations. The roles of collagen fibril bridging and microcracking are relatively insignificant. Based on this appreciation of the toughening mechanisms in bone, the anisotropy in the fracture toughness of bone with orientation can be understood in terms of a large contribution from crack deflection in the transverse orientation as compared to a smaller contribution from crack bridging in the longitudinal orientations.

Acknowledgments

This work was supported in part by the National Institutes of Health under Grant No. 5R01 DE015633 (for RKN), by the Office of Science, Office of Basic Energy Science of the Department of Energy under Contract No. DE-AC03-76SF00098 (for ROR), and by the Laboratory Science and Technology Office, LLNL, under the auspices of the US Department of Energy W-7405-ENG48 (for JSS and JHK). The authors wish to thank Drs. C. M. Puttlitz and Z. Xu (Department of Orthopedic Surgery, University of California, San Francisco, CA, USA) for supply of the human cortical bone used in this study, Dr. J. J. Kruzic (Materials Sciences Division, Lawrence Berkeley National Laboratory, Berkeley, CA, USA) for many useful discussions, and Dr. A. P. Tomsia (Materials Sciences Division, Lawrence Berkeley National Laboratory, Berkeley, CA, USA) for his continued support and encouragement.

References

Ashman, R.B., Rho, J.Y., 1988. Elastic modulus of trabecular bone material. Journal of Biomechanics 21, 177–181.

ASTM Standard E 399-90 (Reapproved 1997), 2001. Annual Book of ASTM Standards, vol. 03.01: Metals— Mechanical testing; Elevated and low-temperature tests; Metallography. ASTM, West Conshohocken.

Behiri, J.C., Bonfield, W., 1989. Orientation dependence on fracture mechanics of bone. Journal of Biomechanics 22, 863–872.

Bilby, B.A., Cardew, G.E., Howard, I.C., 1978. Stress intensity factors at the tips of kinked and forked cracks. In: Fracture 1977, vol. 3. Pergamon Press, Oxford, pp. 197–200.

Burnstein, A.H., Reilley, D.T., Martens, M., 1976. Ageing of bone tissue: Mechanical properties. Journal of Bone and Joint Surgery 58A, 82–86.

Burr, D.B., 2002. The contribution of the organic matrix to bone's material properties. Bone 31, 8–11.

Campbell, J.P., Venkateswara Rao, K.T., Ritchie, R.O., 1999. The effect of microstructure on fracture toughness and fatigue crack growth behaviour in γ-titanium aluminide based intermetallics. Metallurgical and Materials Transactions A 30A, 563–577.

Cotterell, B., Rice, J.R., 1980. Slightly curved or kinked cracks. International Journal of Fracture 16, 155–169.

Currey, J.D., 2001. Sacrificial bonds heal bone. Nature 414, 699.

Evans, A.G., Faber, K.T., 1984. Crack-growth resistance of microcracking brittle materials. Journal of the American Ceramic Society 67, 255–260.

Evans, A.G., McMeeking, R.M., 1986. On the toughening of ceramics by strong reinforcements. Acta Metallurgica 34, 2435–2441.

Ford, C.M., Keaveny, T.M., 1996. The dependence of shear failure properties of trabecular bone on apparent density and trabecular orientation. Journal of Biomechanics 29, 1309–1317.

Govindjee, S., Kay, G.J., Simo, J.C., 1995. Anisotropic modelling and numerical simulation of brittle damage in concrete. International Journal for Numerical Methods in Engineering 38, 3611–3633.

Griffiths, J.R., Owen, D.R.J., 1971. An elastic–plastic stress analysis for a notched bar in plane strain bending. Journal of the Mechanics and Physics of Solids 19, 419–431.

Habelitz, S., Marshall, G.W., Balooch, M., Marshall, S.J., 2002. Nanoindentation and the storage of teeth. Journal of Biomechanics 35, 995–998.

Hill, R., 1950. The Mathematical Theory of Plasticity. Clarendon Press, Oxford.

Hutchinson, J.W., 1987. Crack tip shielding by micro-cracking in brittle solids. Acta Metallurgica 35, 1605–1619.

Katz, J.L., 1980. The structure and biomechanics of bone. Symposium of the Society for Experimental Biology 34, 137–168.

Keaveny, T.M., Wachtel, E.F., Ford, C.M., Hayes, W.C., 1994. Differences between the tensile and compressive strengths of bovine tibial trabecular bone depends on modulus. Journal of Biomechanics 27, 1137–1146.

Lindahl, O., Lindgren, A.G., 1967. Cortical bone in man I. Variation of the amount and density with age and sex. Acta Orthopaedica Scandinavica 38, 133–140.

Lucksanambool, P., Higgs, W.A.J., Higgs, R.J.E.D., Swain, M.W., 2001. Fracture toughness of bovine bone, influence of orientation and storage media. Biomaterials 22, 3127–3132.

Maker, B.N., Hallquist, J.O., 1995. NIKE-3D—a nonlinear, implicit, three-dimensional finite element code for solid and structural mechanics—user's manual, UCRL-MA-105268-REV-1. Lawrence Livermore National Laboratory, Livermore.

Nalla, R.K., Kinney, J.H., Ritchie, R.O., 2003a. Mechanistic fracture criteria for the failure of human cortical bone. Nature Materials 2, 164–168.

Nalla, R.K., Kinney, J.H., Ritchie, R.O., 2003b. On the fracture of human dentin: Is it stress- or strain-controlled? Journal of Biomedical Materials Research 67A, 484–495.

Nalla, R.K., Kinney, J.H., Ritchie, R.O., 2003c. Effect of orientation on the in vitro fracture toughness of dentin: The role of toughening mechanisms. Biomaterials 24, 3955–3968.

Nalla, R.K., Kruzic, J.J., Kinney, J.H., Ritchie, R.O., 2005. Mechanistic aspects of fracture and R-curve behavior in human cortical bone. Biomaterials 26, 217–231.

Nalla, R.K., Kruzic, J.J., Ritchie, R.O., 2004. On the origin of the toughness of mineralized tissue: Microcracking or crack bridging. Bone 34, 790–798.

Nicolella, D.P., Nicholls, A.E., Lankford, J., Davy, D.T., 2001. Machine vision photogrammetry: a technique for measurement of microstructural strain in cortical bone. Journal of Biomechanics 34, 135–139.

Niebur, G.L., Feldstein, M.J., Yuen, J.C., Chen, T.J., Keaveny, T.M., 2000. High-resolution finite element models with tissue strength asymmetry accurately predict failure of trabecular bone. Journal of Biomechanics 33, 1575–1583.

Park, J.B., Lakes, R.S., 1992. Biomaterials: An Introduction. Plenum Press, New York.

Parsamian, G.P., Norman, T.L., 2001. Diffuse damage accumulation in the fracture process zone of human cortical bone specimens and its influence on fracture toughness. Journal of Materials Science 12, 779–783.

Phelps, J.B., Hubbard, G.B., Wang, X., Agrawal, C.M., 2000. Microstructural heterogeneity and the fracture toughness of bone. Journal of Biomedical Materials Research 51, 735–741.

Ritchie, R.O., 1988. Mechanisms of fatigue crack propagation in metals, ceramics and composites: role of crack-tip shielding. Materials Science and Engineering 103, 15–28.

Ritchie, R.O., 1999. Mechanisms of fatigue-crack propagation in ductile and brittle solids. International Journal of Fracture 100, 55–83.

Shang, J.-K., Ritchie, R.O., 1989. Crack bridging by uncracked ligaments during fatigue-crack growth in SiC-reinforced aluminum-alloy composites. Metallurgical Transactions A 20A, 897–908.

Sigl, L.S., 1996. Microcrack toughening in brittle materials containing weak and strong interfaces. Acta Materialia 44, 3599–3609.

Simo, J.C., Ju, J.W., 1987. Strain- and stress-based continuum damage models-I. Formulation. International Journal of Solids and Structures 23, 821–840.

Stölken, J.S., Kinney, J.H., 2003. On the importance of geometric nonlinearity in finite-element simulations of trabecular bone failure. Bone 33, 494–504.

Taylor, D., 2003. How does bone break? Nature Materials 2, 133–134.

Thompson, J.B., Kindt, J.H., Drake, B., Hansma, H.G., Morse, D.E., Hansma, P.K., 2001. Bone indentation recovery time correlates with bond reforming time. Nature 414, 773–776.

Vashishth, D., Behiri, J.C., Bonfield, W., 1997. Crack growth resistance in cortical bone: Concept of microcrack toughening. Journal of Biomechanics 30, 763–769.

Vashishth, D., 2000. In vivo diffuse damage in human vertebral trabecular bone. Bone 26, 147–152.

Vashishth, D., Tanner, K.E., Bonfield, W., 2000. Contribution, development and morphology of microcracking in cortical bone during crack propagation. Journal of Biomechanics 33, 1169–1174.

Wang, X., Bank, R.A., Tekoppele, J.M., Agrawal, C.M., 2001. The role of collagen in determining bone mechanical properties. Journal of Orthopaedic Research 19, 1021–1026.

Wang, X., Shen, X., Li, X., Agrawal, C.M., 2002. Age-related changes in the collagen network and the toughness of bone. Bone 31, 1–7.

Wright, T.M., Hayes, W.C., 1976. The fracture mechanics of fatigue crack propagation in compact bone. Journal of Biomedical Materials Research 10, 637–648.

Yeh, O.C., Keaveny, T.M., 2001. Relative roles of microdamage and microfracture in the mechanical behavior of trabecular bone. Journal of Orthopaedic Research 19, 1001–1007.

Yeni, Y.N., Norman, T.L., 2000. Calculation of porosity and osteonal cement line effects on the effective fracture toughness of cortical bone in longitudinal crack growth. Journal of Biomedical Materials Research 51, 504–509.

Yeni, Y.N., Fyhrie, D.P., 2001. Collagen-bridged microcrack model for cortical bone tensile strength. In: Proceedings of the 2001 Summer Bioengineering Conference, BED-vol. 50. ASME, New York, pp 293–294.

Zioupos, P., Currey, J.D., 1998. Changes in the stiffness, strength, and toughness of human cortical bone with age. Bone 22, 57–66.